International Journal of Electrical and Computer Engineering (IJECE)
Vol. 16, No. 3, June 2026, pp. 1097~1106
ISSN: 2088-8708, DOI: 10.11591/ijece.v16i3.pp1097-1106

Flashover of a polluted high voltage insulator under electric field distribution

Zainab Abdullah[1], Izham Zainal Abidin[1], Miszaina Osman[1], Nurulazmi Abd. Rahman[2], Muhammad Shafiq[3]
[1]Department of Electrical Engineering, College of Engineering, Universiti Tenaga Nasional, Putrajaya, Malaysia
[2]School of Microelectronic Engineering, Universiti Malaysia Perlis, Arau Perlis, Malaysia
[3]Center for Advanced Power Systems, Florida State University, Tallahassee, United State

Article Info

Article history:

Received Oct 1, 2024
Revised Feb 23, 2026
Accepted Mar 16, 2026

Keywords:

2D axisymmetric simulation
COMSOL Multiphysics
Electric field distribution
Flashover
High voltage glass insulators
Surface pollution

ABSTRACT

This study investigates the effect of surface pollution on a single-unit 11 kV glass suspension insulator using two-dimensional (2D) axisymmetric simulations in COMSOL Multiphysics. The developed model incorporates the electrical properties of glass, cement, steel electrodes, surrounding air, and a uniform pollution layer, with an applied AC voltage of 11 kV under quasi-static conditions. Simulation results demonstrate pronounced electric field intensification in the polluted configuration, particularly at the air–glass–cap triple junction region, where localized electrical stress is significantly higher compared to the clean condition. While the clean insulator operates within IEC 60383 recommended limits, the polluted model exhibits elevated peak electric field magnitudes, indicating increased flashover vulnerability. The findings highlight the strong influence of surface contamination, material permittivity, and geometric configuration on electric field distribution along the creepage path. This study establishes a reliable and computationally efficient predictive framework for optimizing insulator design, improving maintenance strategies, and enhancing the long-term reliability of high-voltage transmission systems, especially in pollution-prone environments.

Corresponding Author:

Zainab Abdullah
Department of Electrical Engineering, College of Engineering, Universiti Tenaga Nasional
Putrajaya Campus, 43000 Kajang, Selangor Malaysia
Email: zainabmrsabdullah@gmail.com

1. INTRODUCTION

High-voltage glass insulators, an earlier development of ceramic insulators, continue to be widely used in transmission line systems due to their robust mechanical strength, strong resistance to electrical stress, and durability under adverse environmental conditions [1], [2]. These insulators provide essential protection by preventing unwanted current flow through equipment and ensuring operational safety for personnel [3]. In addition, high-voltage glass insulators demonstrate excellent resistance to material degradation caused by electrical stress and discharge activities [4]–[6]. Constructed from toughened glass and galvanized steel components, they are commonly referred to as cap-and-pin insulators [7]. These insulators are typically arranged in suspension or tension strings on transmission towers, where the number of units per string varies according to system voltage levels, such as 3–4 units for 33 kV, 5 units for 66 kV, and 6–12 units for 132 kV applications [8]–[11].

Despite their advantages, high-voltage glass insulators remain susceptible to environmental influences, particularly surface pollution, which can degrade their electrical performance. The deposition of pollutants on the insulator surface may initiate material deterioration and arc discharge activity, leading to increased electric field stress and a higher probability of flashover. Previous studies have reported that environmental conditions significantly influence insulator properties, where the combined presence of pollutants and moisture contributes to increased surface conductivity and potential flashover events [12]–[18]. Research on pollution distribution under various contaminant types has demonstrated that flashover may occur when deposited pollutants become wet, forming a conductive layer along the insulator surface [19]. This conductive layer facilitates leakage current flow, thereby reducing surface resistivity and increasing electrical stress. Generally, the greater the pollution severity on the insulator surface, the higher the surface conductivity and the greater the likelihood of flashover [20], [21]. Shea [22] also highlighted pollution flashover problems under unfavorable environmental conditions, while other researchers have utilized humidity and temperature indicators to evaluate flashover behavior in transmission insulators [23].

Leakage current analysis has been widely adopted as a method to predict flashover occurrences [24], [25]. The leakage distance of insulation is influenced by the type of pollution and the insulation material properties. Higher electric field magnitudes are strongly correlated with increased flashover risk due to accelerated charge movement and reduction of surface resistivity. As resistivity decreases, leakage current increases along the creepage path. Yang *et al.* [26] similarly emphasized that leakage performance depends on both contamination severity and insulation characteristics. However, although numerous studies have focused on polluted insulators, several challenges remain. Experimental investigations are often constrained by safety risks, equipment limitations, and difficulties in directly measuring electric field magnitudes under high-voltage conditions. Furthermore, non-uniform heating and localized voltage drops complicate the accurate interpretation of electric field characteristics, limiting comprehensive understanding of stress distribution along the insulator surface. To address these limitations, simulation techniques, particularly the finite element method (FEM), provide an effective alternative for evaluating electric field stress in high-voltage insulation systems. FEM is a powerful computational approach capable of predicting electric potential and field distribution with high accuracy, enabling detailed investigation of stress concentration and flashover mechanisms [27]–[35]. Through numerical modeling, the electric field distribution along the creepage distance of cap-and-pin glass insulators can be analyzed under different pollution conditions, including variations in pollution layer thickness.

Therefore, this study aims to further investigate the effect of surface pollution on electric field distribution along the creepage distance of a single-unit 11 kV glass suspension insulator using a two-dimensional (2D) axisymmetric simulation model. The analysis considers independent and dependent variables including electric field distribution, potential distribution, temperature influence, and leakage current, with key parameters such as relative permittivity (εr) and conductivity (σ). The findings of this work are expected to contribute to improved insulator design, optimized maintenance strategies, and enhanced reliability of transmission systems, particularly in supporting the expansion of renewable energy infrastructure.

2. METHOD

A two-dimensional (2D) model of the insulator was developed using AutoCAD software, chosen for its efficiency and precision in creating detailed engineering designs. While both 2D and three-dimensional (3D) modeling options are available, 2D modeling is often preferred for its simplicity and reduced computational requirements, making it more accessible for initial design stages.

2.1. Geometry development of glass insulator

A 2D axisymmetric model of a single-unit 11 kV glass suspension insulator was developed in AutoCAD and subsequently imported into COMSOL Multiphysics (version 5.0) for numerical simulation. The sample of a single-unit 11 kV glass insulator is shown in Figure 1. The 2D axisymmetric model was designed using AutoCAD. This approach is commonly used in high-voltage insulator analysis due to its efficiency in handling rotationally symmetric geometries and significantly reduces computational time while maintaining high accuracy in representing the electric field distribution along the insulator profile. The 2D insulator model comprises five distinct regions which U1: Pin (steel), U2: Cement between cap and glass, U3: Glass dielectric body, U4: Cement between glass and cap, U5: Cap (steel). These regions were carefully defined as separate domains to enable accurate assignment of material properties as depicted in Figure 2. The 2D model design was extruded into a 3D insulator model, as illustrated in Figure 3. Figure 3(a) 3D extruded model in combined layers. Figure 3(b) generated 3D glass insulator model shows the finalized geometry that was verified the continuity and absence of overlapping or disconnected boundaries before simulation. The geometrical dimensions were adopted according to IEC 60383 standards. The parameters of the insulator are summarized in Table 1. The dimensions of a single-unit 11 kV glass insulator with possesses a diameter (D) of 255 mm, a height (H) of 127 mm, and a nominal creepage distance (L) of 320 mm. These dimensions serve as the foundational parameters for the initial model design [36]. Modifications to accommodate specific simulation requirements were implemented to improve measurement accuracy and performance in the analysis. The surrounding air domain was extended to at least three times the insulator diameter to minimize boundary effects and ensure accurate electric field computation.

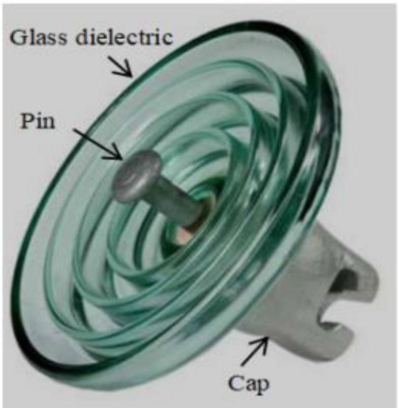

Figure 1. Glass insulator in actual view

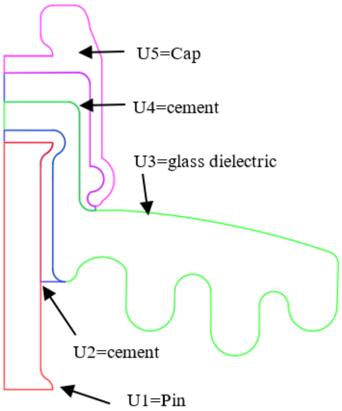

Figure 2. 2D insulator model in layer domain

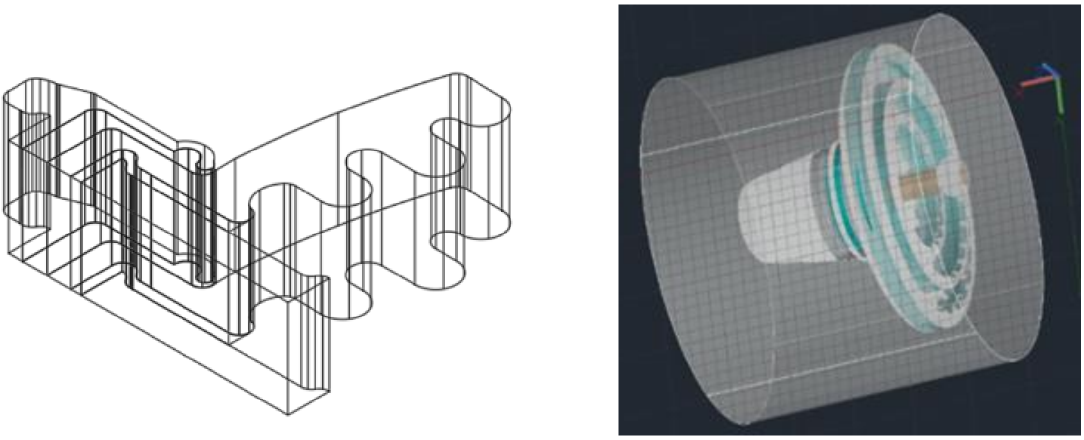
(a) (b)

Figure 3. 3D extruded model in (a) combined layers and (b) generated 3D glass insulator model

Table 1. Dimensions of a single-unit 11kV glass insulator

Material	Diameter (D, mm)	Height (H, mm)	Nominal creepage distance (L, mm)
Glass	255	127	320

2.2. Simulation setup in COMSOL

The imported geometry was solved using the electrostatics interface under the AC/DC module in COMSOL Multiphysics. Two surface conditions were analyzed for ii) clean surface (CS) and ii) surface polluted (SP). The measurement of the creepage distance along the insulator surface, spanning from point x to point y as shown in Figure 4. For the polluted model, a uniform contamination layer with a thickness of 1.5 mm and length of 43 mm was applied along the insulator surface. The governing relationship for the electric field distribution is expressed as in (1):

$$E = -\nabla . V \tag{1}$$

where E represents the electric field intensity (V/m), ∇ is the rate of change and V is the voltage potential (V).

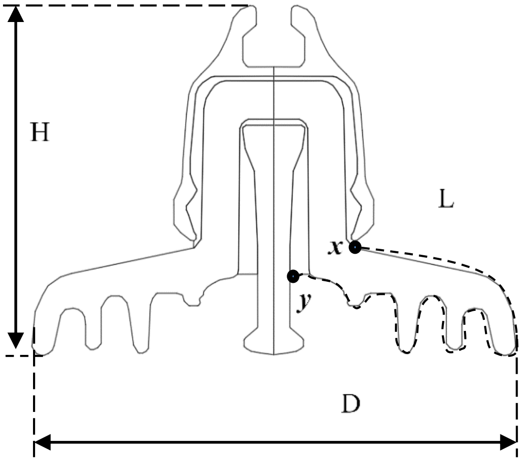

Figure 4. Creepage distance (x to y with dotted line)

2.2.1. Boundary conditions

The high-voltage line of the AC voltage was applied to the pin, and the cap was connected to the ground electrode terminal to protect the flow of current to the ground through the tower structure. The simulation was performed under quasi-static, steady-state conditions at a power frequency of 50 Hz, where displacement current dominates and magnetic effects are negligible. The outer boundary of the air domain was assigned electric insulation boundary conditions to emulate an open-space environment without external field interference. The peak voltage value was selected to evaluate the maximum electric stress experienced by the insulator surface, as electric field intensity is directly proportional to the applied potential. This approach ensures conservative assessment under worst-case operating conditions.

2.2.2. Meshing strategy

In COMSOL Multiphysics, mesh generation involves subdividing the simulation domain into smaller elements, typically triangular in two-dimensional models, to facilitate numerical analysis. A physics-controlled fine mesh was implemented, with local mesh refinement applied at triple junction regions, creepage surface and pollution layer interface. Mesh independence analysis was conducted to confirm that variations in mesh density did not significantly affect the maximum electric field values.

2.2.3. Electric field evaluation

The electric field distribution along the insulator surface was evaluated for both CS and SP conditions as represented in Figure 5. The normalized electric field magnitude was extracted to analyze stress concentration regions. Figure 5(a) shows the CS model, and Figure 5(b) shows the SP model with the pollution layer. The blue line indicates the creepage distance along the insulator surface, which is critical for analyzing the electric field distribution. The electromagnetic properties assigned to each domain, as shown in Figure 2, are listed in Table 2. The relative permittivity, εr of the glass dielectric (U3) is assigned a value of 4.2. The steel (U1 and U5) is set up as 1.0, and the cement (U2 and U4) is taken as 2.09. The air around the insulators has a specified permittivity of 1.0. The relative permittivity of 81 indicates that the model is uniformly distributed, with a pollution layer on the surface. The air region borders characteristic physical system in a solitary, open space with electromagnetic sources and an anticipated zero external current.

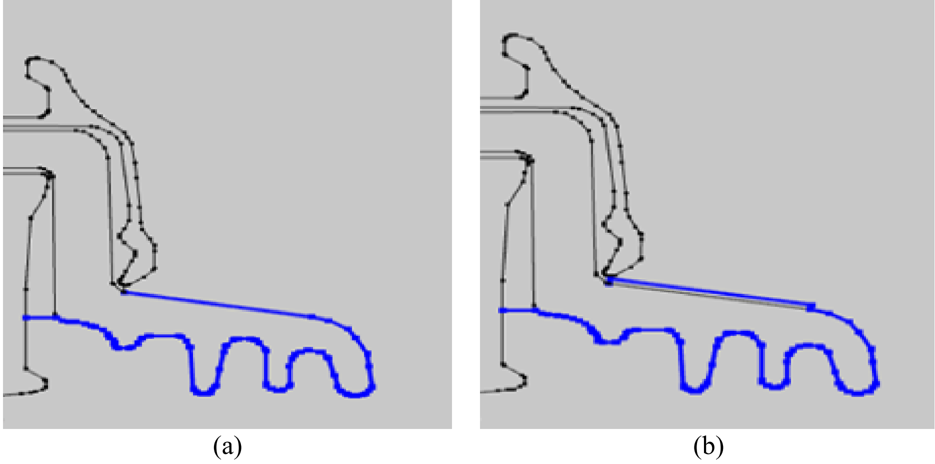
(a) (b)

Figure 5. Simulation models in (a) clean surface (CS) and (b) polluted surface (SP)

Table 2. Electromagnetic properties of materials

Material	Relative permittivity (εr)
Steel (U1, U5)	1.0 (modeled as PEC)
Glass (U3)	4.2
Cement (U2, U4)	2.09
Air	1.0
Pollution layer	81

3. RESULTS AND DISCUSSION

The modeling stages, simulations conducted on both clean and polluted insulators, and subsequent data analysis are critical phase in this study. The simulated maximum electric field values for both CS and SP models were compared with the IEC 60383 recommended values. The CS model stayed within safe limits, confirming that the insulator design meets international standards. The SP model showed localized enhancement of the electric field due to pollution, suggesting that insulator cleaning or design adjustments may be necessary in high-pollution environments.

3.1. Meshing discretization

Figure 6(a) and 6(b) presents the meshing discretization for both CS and SP conditions. This process is crucial, especially in regions where material properties exhibit significant variability, as it ensures accurate representation of the geometry and boundary conditions. The generated mesh defines the computational framework for the model, delineating boundaries and influencing the precision of the simulation results. A finer mesh, characterized by smaller elements, can capture detailed variations in the electric field more accurately but requires increased computational resources and time. Conversely, a coarser mesh reduces computational load but may compromise result accuracy. Therefore, selecting an appropriate mesh size involves balancing the need for precision with computational efficiency. The number of mesh elements is inherently dependent on the actual size and complexity of the model geometry.

3.2. Comparison of the electric field distribution between clean and polluted surfaces

The simulation results of the electric field distribution for both clean and polluted insulator surfaces are shown in Figure 7. In Figure 7(a), the equipotential contour lines for the clean surface condition are depicted, with blue representing the lowest potential values and red indicating the highest. This analysis validates the accuracy of the insulator model and serves as a reference for further studies. This analysis also helps to enhance the validity of the insulator model for further analysis. For the CS model, the maximum electric field intensity was observed near the triple junction region between the pin, glass, and air, consistent with high-stress regions reported in previous studies. The peak value did not exceed the IEC 60383 recommended withstand limit for a single-unit 11 kV insulator, confirming the design adequacy under normal operating conditions. The electric field distribution for the surface polluted (SP) condition as illustrates in Figure 7(b) shows that the presence of a pollution layer (thickness=1.5 mm, length=43 mm) significantly altered the electric field distribution. The electric field magnitude increased at the surface of the pollution layer, with peak values concentrated at the interface between the pollution layer and the glass surface, specifically at points A, B, and C. This indicates that contamination enhances local electric stress, which could potentially trigger surface flashover under extreme conditions. Notably, elevated electric field intensities are observed at internal regions of the electrodes. These localized enhancements suggest that pollution significantly influences the electric field distribution, potentially increasing the risk of surface flashover.

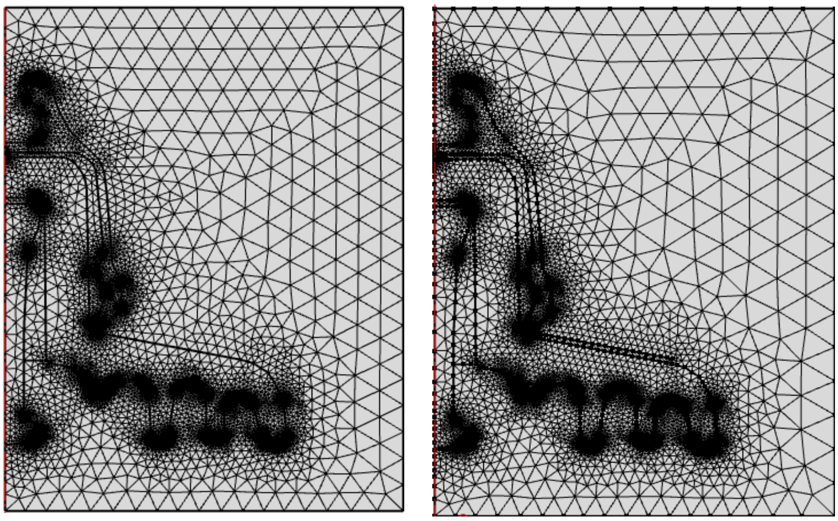

(a) (b)

Figure 6. Meshing discretization in (a) CS insulator and (b) SP insulator

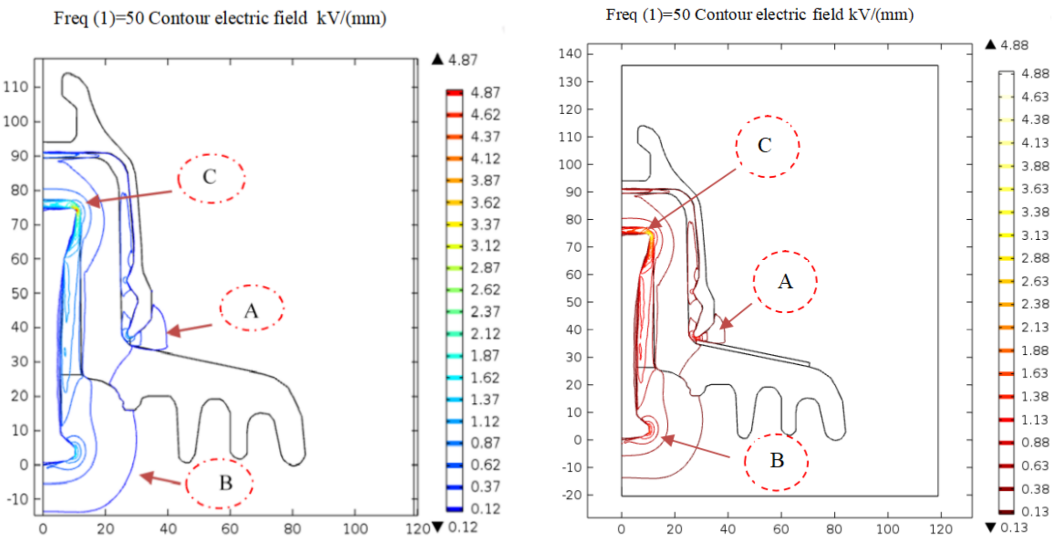

(a) (b)

Figure 7. Contour electric field distribution in (a) a clean insulator and (b) a polluted insulator

The simulation results of the electric field distribution for both clean surface (CS) and surface polluted (SP) conditions are discussed in Figure 8. In the chart, the CS condition is represented by a blue line, while the SP condition is depicted by a red line. From Figure 8, it can be seen that in Region I, both models exhibit a peak electric field intensity near the cap, approximately 1 kV/mm. In Region II, the electric field demonstrates a decelerating trend with noticeable undulations between the ground end (0 V) and the high-voltage end (11 kV), particularly between 20 mm and 40 mm along the creepage distance. Region III exhibits distinct differences between the CS and SP conditions. The tangential electric field analysis reveals that for the CS model, the electric field is relatively uniform along the creepage path, with minor concentration near triple junctions. However, the SP model shows that the electric field spikes at the pollution layer boundaries, indicating high local stress zones. These findings highlight the critical role of surface contamination in the performance of glass insulators. The results align with previous studies, such as Salhi *et al.* [37] indicating that pollution can reduce the insulator's withstand voltage and increase the risk of flashover. The presence of a pollution layer on the insulator surface alters the electric field distribution, especially at the triple junction of air, cap, and glass interfaces. This alteration facilitates the movement of positive and negative charges between the pollution layer, insulation material, and conductor interface, leading to increased electric field magnitudes and can promote localized surface heating, primarily near the end-fitting regions, and may precipitate flashover events. If the electric field intensity exceeds 4.5 kV/mm, the likelihood of insulator flashover significantly increases. These observations corroborate the theoretical discussions presented in section 1.

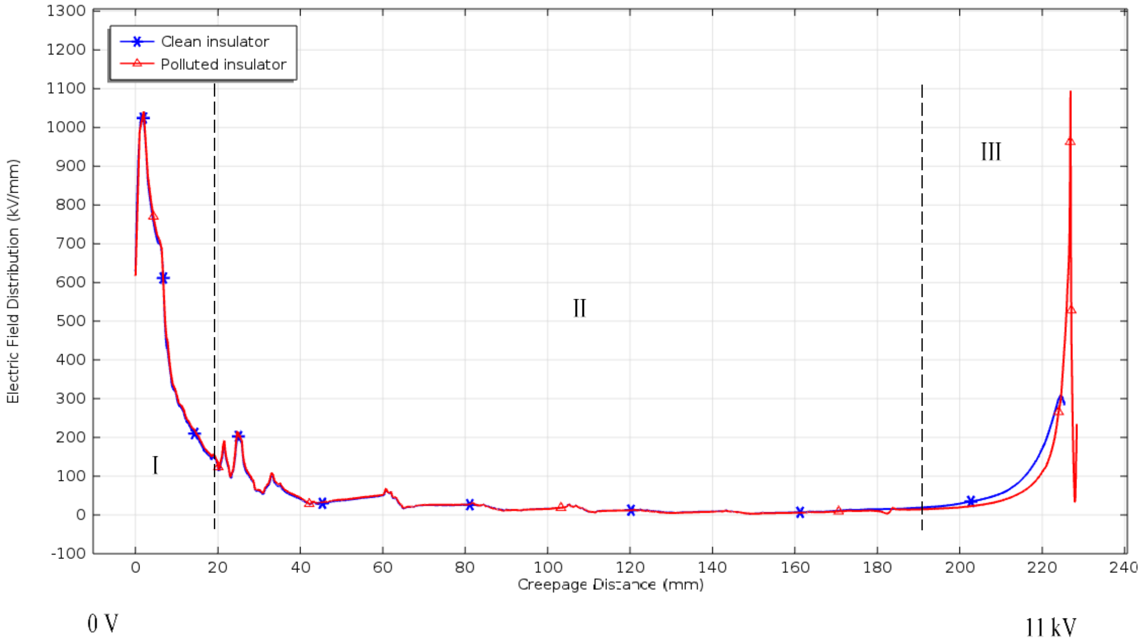

Figure 8. Normalized electric field along the creepage path for CS and SP surfaces

3.3. Effect of geometrical and material properties

The simulation demonstrates that the geometry of the insulator (diameter, creepage distance, triple junction regions) significantly affects the electric field distribution. The material properties of glass (εr=4.2), cement (εr=2.09), and steel (1.0) determine the distributed field across the insulator surface and internal regions. It can be suggested that increasing the creepage distance reduces the peak surface electric field. The high relative permittivity of the pollution layer (εr=81) concentrates the field at the layer edges, consistent with theoretical predictions from electrostatics.

4. CONCLUSION

This study presents a 2D axisymmetric simulation of a single-unit 11 kV glass suspension insulator under both clean and polluted surface conditions using COMSOL Multiphysics. The study emphasizes that surface contamination significantly affects electric field distribution and insulator performance. Proper insulator geometry and material selection are crucial for minimizing electric stress. In conclusion, simulation using COMSOL 2D axisymmetric models provides a reliable tool to predict field distribution prior to experimental validation. A well-constructed model facilitates efficient and accurate simulations. Inaccurate parameter data can prolong simulation times and complicate the analysis of results. Parameters such as dimensions, pollution layer thickness, and material permittivity significantly influence the correlation between electric field distribution and flashover occurrences. Therefore, adjustments of insulator dimensions are crucial to enhance design efficacy. The analysis of the two cases in clean and polluted insulators relates to electric field intensity and hotspot formation along the creepage distances along the insulator surface. These results provide practical guidance for maintenance and geometry on insulator performance of high-voltage transmission lines, particularly in regions with high pollution levels. Implementing appropriate design enhancements and selecting suitable material properties can mitigate the adverse effects of pollution, thereby enhancing the reliability and longevity of power transmission systems.

ACKNOWLEDGEMENTS

The authors would like to thank UNITEN for their cooperation in this study.

FUNDING INFORMATION

Authors state no funding involved.

CONFLICT OF INTEREST STATEMENT

Authors state no conflict of interest.

DATA AVAILABILITY

Data availability is not applicable to this paper as no new data were created or analyzed in this study.

REFERENCES

[1] M. A. Alston, “Porcelain and glass insulator in high voltage application,” *Journal of Electrical Insulation*, vol. 28, no. 4, pp. 324–330, 2019.

[2] S. Khan, S. Alam, and M. Z. Saleem, “Analysis of electric field and leakage current of glass and porcelain insulators under clean and polluted conditions: A comparative study of three profiles,” *Electric Power Systems Research*, vol. 239, p. 111283, 2025, doi: 10.1016/j.epsr.2024.111283.

[3] J. S. T. Looms, *Insulators for High Voltages*. Peter Peregrinus Ltd., 1988, doi: 10.1049/pbpo007e.

[4] L. L. Grigsby, *Electric power generation, transmission, and distribution: The electric power engineering handbook*, 3rd ed. CRC Press, 2012.

[5] W. D. Metz, *High voltage engineering: accelerating away from science*, vol. 177, no. 4044. Butterworth-Heinemann, 1972, doi: 10.1126/science.177.4044.151.

[6] A. P. Mishra, R. S. Gorur, and S. Venkataraman, “Evaluation of porcelain and toughened glass suspension insulators removed from service,” *IEEE Transactions on Dielectrics and Electrical Insulation*, vol. 15, no. 2, pp. 467–475, 2008, doi: 10.1109/TDEI.2008.4483466.

[7] Global Insulator Group, “Glass insulators for 10 – 1150 kV overhead lines and substations - Products catalogue,” *Global Insulator Group*. pp. 1–16, 2021.

[8] S. F. M. Nor, M. Z. A. Ab Kadir, A. M. Ariffin, M. Osman, M. S. A. Rahman, and N. M. Zainuddin, “Systematic approaches and analyses on voltage uprating of 132 kv transmission lines: A case study in malaysia,” *Applied Sciences (Switzerland)*, vol. 11, no. 19, 2021, doi: 10.3390/app11199087.

[9] H. Rahman, M. S. Hossain, and M. M. Hasan, “A overview of A 132 / 33 KV substation,” Thesis, Faculty of Engineering, Daffodil International University, 2020.

[10] M. Othman, M. Isa, M. N. Mazlee, M. A. M. Piah, and N. A. Rahman, “Simulation of 33 kV string insulators using finite element method (FEM),” in *2019 IEEE Student Conference on Research and Development, SCOReD 2019*, 2019, pp. 86–89, doi: 10.1109/SCORED.2019.8896273.

[11] K. Holtzhausen and W. Vosloo, *High voltage engineering - Practice and Theory*. 2011.

[12] S. Satta, A. Bayadi, and R. Boudissa, “Alternating current flashover voltage of a uniform polluted glass flat insulator under parallel electric discharges effect,” *International Journal of Electrical and Computer Engineering*, vol. 12, no. 4, pp. 3454–3465, 2022, doi: 10.11591/ijece.v12i4.pp3454-3465.

[13] M. T. Gencoglu, “The comparison of ceramic and non-ceramic insulators,” *e-journal of New World Sciences Academy*, vol. 2, no. 4, pp. 275–294, 2007.

[14] M. P. Lalitha, K. V. P. Kumar, and V. Samala, “Design and simulation of voltage and electric field distribution on disc insulators using finite element method in Opera software,” in *2014 International Conference on Smart Electric Grid, ISEG 2014*, 2015, pp. 1–6, doi: 10.1109/ISEG.2014.7005587.

[15] S. Hardi, Y. Tarigan, H. Zulkarnaen, and A. Hasibuan, “Influence of artificial pollutants on disc insulators under dry and wet conditions on leakage current and flashover voltage,” in *2019 3rd International Conference on Electrical, Telecommunication and Computer Engineering, ELTICOM 2019 - Proceedings*, 2019, pp. 174–178, doi: 10.1109/ELTICOM47379.2019.8943858.

[16] H. Nouir-Masmoudi and N. Dhahbi-Megriche, “Effect of pollution layer discontinuity due to the dry bands presence on potential and electric field along insulator,” in *Proceedings of the 2022 5th International Conference on Advanced Systems and Emergent Technologies, IC_ASET 2022*, 2022, pp. 233–238, doi: 10.1109/IC_ASET53395.2022.9765860.

[17] J. A. Araújo *et al.*, “A case study of glass insulator pin failure in 500 kV transmission line,” *Engineering Failure Analysis*, vol. 153, pp. 1–19, 2023, doi: 10.1016/j.engfailanal.2023.107582.

[18] A. A. Salem *et al.*, “Influence of contamination distribution in characterizing the flashover phenomenon on outdoor insulator,” *Ain Shams Engineering Journal*, vol. 14, no. 12, p. 102249, 2023, doi: 10.1016/j.asej.2023.102249.

[19] M. G. Gebremichael, J. M. Bikorimana, and J. Desmet, “Flashover voltage variations of glass and porcelain insulators with different contaminants,” in *2022 IEEE PES/IAS PowerAfrica, PowerAfrica 2022*, 2022, pp. 1–4, doi: 10.1109/PowerAfrica53997.2022.9905277.

[20] I. Ramirez, R. Hernández, and G. Montoya, “Measurement of leakage current for monitoring the performance of outdoor insulators in polluted environments,” *IEEE Electrical Insulation Magazine*, vol. 28, no. 4, pp. 29–34, 2012, doi: 10.1109/MEI.2012.6232007.

[21] A. A. Salem, R. Abd-Rahman, S. A. Al-Gailani, M. S. Kamarudin, H. Ahmad, and Z. Salam, “The leakage current components as a diagnostic tool to estimate contamination level on high-voltage insulators,” *IEEE Access*, vol. 8, pp. 92514–92528, 2020, doi: 10.1109/ACCESS.2020.2993630.

[22] J. Shea, “Advances in High Voltage Engineering [Book Review],” *IEEE Electrical Insulation Magazine*, vol. 23, no. 1, pp. 53–53, 2007, doi: 10.1109/mei.2007.288471.

[23] S. Amalia *et al.*, “The effect of humidity and temperature on flashover in high-voltage transmission line ceramic insulators,” *TEM Journal*, vol. 13, no. 1, pp. 670–680, Feb. 2024, doi: 10.18421/TEM131-70.

[24] A. A. Salem *et al.*, “Pollution flashover characteristics of coated insulators under different profiles of coating damage,” *Coatings*, vol. 11, no. 10, p. 1194, 2021, doi: 10.3390/coatings11101194.

[25] M. Junaid, J. Wang, H. Li, B. Xiang, Z. Liu, and Y. Geng, “Flashover characteristics of vacuum interrupters in liquid nitrogen and its comparison with air and transformer oil for the superconducting switchgear applications,” *International Journal of Electrical Power and Energy Systems*, vol. 125, p. 106504, 2021, doi: 10.1016/j.ijepes.2020.106504.

[26] Z. Yang, X. Jiang, Z. Zhang, D. Zhang, and Y. Liu, “Electrical property of different types insulator string under typical pollution constituents,” in *Annual Report - Conference on Electrical Insulation and Dielectric Phenomena, CEIDP*, 2015, vol. 2015-December, pp. 170–175, doi: 10.1109/CEIDP.2015.7352025.

[27] COMSOL, *COMSOL Multiphysics Version 5.1*, CM010001, 2015.

[28] L. Wang, J. Chong, N. Dang, J. Zhao, and J. Zhao, “Research about the thermoelectric coupling of insulator surface dry band and COMSOL simulation,” in *IET Conference Proceedings*, 2020, vol. 2020, no. 1, pp. 1593–1599, doi: 10.1049/icp.2020.0370.

[29] A. F. Cadena, J. S. Mendoza, and H. F. Ibáñez, “COMSOL modeling of the lightning-generated electric field distribution in a chain of insulators of a 115 kV power transmission line,” in *Journal of Physics: Conference Series*, 2021, vol. 2135, no. 1, pp. 1–11, doi: 10.1088/1742-6596/2135/1/012006.

[30] I. Mohamed, K. Aramugam, and M. K. A. A. Khan, “Simulation and measurement of the voltage distribution on porcelain insulator string under polluted condition,” in *2018 IEEE 4th International Symposium in Robotics and Manufacturing Automation, ROMA 2018*, 2018, pp. 1–5, doi: 10.1109/ROMA46407.2018.8986724.

[31] A. S. Krzma, M. Y. Khamaira, and M. Abdulsamad, “Comparative analysis of electric field and potential distributions over porcelain and glass insulators using finite element method,” in *Proceedings of First Conference for Engineering Sciences and Technology (CEST-2018)*, 2018, vol. 1, pp. 176–184, doi: 10.21467/proceedings.2.22.

[32] M. Jenithra, G. Sudalaimani, E. Raja Sekaran, D. Swathi, K. Kumar, and R. V. Maheswari, “Investigation of electric field distribution on a 33kV polymeric insulator under polluted conditions using finite element method,” in *4th International Conference on Circuits, Control, Communication and Computing, I4C 2022*, 2022, pp. 231–235, doi: 10.1109/I4C57141.2022.10057935.

[33] S. Narain, M. F. Khan, and A. Swanson, “Insulator electric fields using FEM software,” in *Proceedings of the 32nd Southern African Universities Power Engineering Conference, SAUPEC 2024*, 2024, pp. 1–6, doi: 10.1109/SAUPEC60914.2024.10445094.

[34] A. Abimouloud, D. Korichi, and S. Arif, “A new dynamic 3D FEM model of arc propagation on cap-and-pin polluted insulator to predict DC flashover voltage,” in *Proceedings of 2016 8th International Conference on Modelling, Identification and Control, ICMIC 2016*, 2017, pp. 898–902, doi: 10.1109/ICMIC.2016.7804242.

[35] T. P. Hong and T. Van Top, “Electrical field behavior of transmission line insulators in polluted area,” in *Proceedings of the International Symposium on Electrical Insulating Materials*, 2008, pp. 530–533, doi: 10.1109/ISEIM.2008.4664475.

[36] H. Benguesmia, N. M’Ziou, and A. Boubakeur, “Simulation of the potential and electric field distribution on high voltage insulator using the finite element method,” *Diagnostyka*, vol. 19, no. 2, pp. 41–52, 2018, doi: 10.29354/diag/86414.

[37] R. Salhi, A. Mekhaldi, M. Teguar, and O. Kherif, “Quantitative analysis of electric charge distribution on cap-pin insulator using COMSOL multiphysics,” in *Fourth International Conference on Technological Advances in Electrical Engineering (ICTAEE’23)*, 2024, pp. 576–579.

BIOGRAPHIES OF AUTHORS

Zainab Abdullah received the B.Eng. and M.Eng. degrees in electrical engineering from Universiti Teknologi Malaysia in 2001 and 2011, respectively. She is also a Professional Engineer (P.Eng.) of the Board of Engineers Malaysia, as well as a member of the Institution of Engineers Malaysia (IEM). Her research interests include high voltage engineering, dielectric materials, and lightning protection. She can be contacted at email: zainabmrsabdullah@gmail.com.

Izham Zainal Abidin received the B.Sc. degree in electrical engineering from the University of Southampton, Southampton, U.K., in 1997, and the Ph.D. degree in electrical engineering from the University of Strathclyde, Glasgow, U.K., in 2002. He is currently a professor with the Department of Electrical Power Engineering and the Vice Chancellor (Academic and International) at Universiti Tenaga Nasional (UNITEN), Selangor. His research interests include power system analysis, artificial intelligence, and smart grid. He can be contacted at email: izham@uniten.edu.my.

Miszaina Osman received the bachelor's degree in electrical engineering from the University of Southampton, U.K., in 1999, and the Ph.D. degree in electrical engineering in 2004. She is currently an associate professor with the Institute of Power Engineering, Universiti Tenaga Nasional (UNITEN). She is also a Professional Engineer (P.Eng.), a Chartered Engineer (C.Eng.), and a member of the Institution of Engineering and Technology (IET), U.K., the Institution of Engineers Malaysia (IEM), the National Mirror Committee of IEC TC81 (Lightning Protection), a country representative for IEC TC81 meetings, and the CIGRE Working Group C4.50 (Evaluation of Transient Performance of Grounding System in Substation). Her research interests include power system grounding, lightning protection, and high voltage. She can be contacted at email: miszaina@uniten.edu.my.

Nurulazmi Abd. Rahman received the B.Eng. in power engineering, M.Eng. in power engineering, and Ph.D. degrees from Universiti Malaysia Perlis (UniMAP). He is currently a senior lecturer with the School of Microelectronic Engineering, UniMAP. He is a Professional Engineer with Practicing Certificate (PEPC) of the Board of Engineers Malaysia and a corporate member of the Institution of Engineers Malaysia. His research interests include high voltage, power system interconnection, power system reliability, and power transmission reliability. He can be contacted at email: nurulazmi@unimap.edu.my.

Muhammad Shafiq received the M.Sc. degree from UET Lahore, Pakistan, in 2007, and the Ph.D. degree in power systems from Aalto University, Finland, in 2014. From 2001 to 2009, he was a lecturer and assistant professor with IUB, Pakistan, and from 2015 to 2017, he was a researcher with industrial organizations in Finland. He was an assistant professor with the Department of Electrical Engineering and Energy Technology, University of Vaasa, Finland, from 2017 to 2020. In 2021, he joined as a senior researcher with Tallinn University of Technology, Estonia. Currently, he is with Florida State University, USA. His research interests include power systems, high-voltage engineering, partial discharge diagnostics, condition monitoring of power system components, and the design of sensors for high-frequency measurements. He can be contacted at email: ms22ds@fsu.edu.